# Ab Initio CASSCF and DFT Investigations of $(H_2O)_2^+$ and $(H_2S)_2^+$: Hemi-Bonded vs Proton-Transferred Structure

**Tapan K. Ghanty* and Swapan K. Ghosh***

*Theoretical Chemistry Section, RC & CD Division, Chemistry Group, Bhabha Atomic Research Centre, Mumbai 400 085, India*

*Received: July 2, 2002; In Final Form: September 12, 2002*

High level ab initio calculations using a complete active space self-consistent field (CASSCF) and multiconfigurational quasi-degenerate perturbation theory (MCQDPT2) methods as well as density functional theory (DFT)-based calculations with different exchange−correlation energy density functionals have been performed for predicting the relative stability of the proton-transferred vs hemi-bonded isomers of $(H_2O)_2^+$ and $(H_2S)_2^+$ species. For $(H_2O)_2^+$, DFT calculation using conventional exchange−correlation functionals predicts the hemi-bonded structure to be the ground state while use of full or half Hartree−Fock exchange and local correlation predicts a higher stability of the proton-transferred structure in agreement with ab initio results. For the $(H_2S)_2^+$ system, all of the methods lead to the prediction of lower energy for the hemi-bonded isomer. No regular trend of the exchange−correlation energy component with the total energy difference is however observed. Dynamical electron correlation effect incorporated through MCQDPT2 is found to be much stronger in $(H_2O)_2^+$ as compared to $(H_2S)_2^+$. An analysis of the nature of interactions involved in the $(H_2O)_2^+$ and $(H_2S)_2^+$ systems within the framework of Bader's topological theory of atoms in molecules is also presented through the plots of the Laplacian $\nabla^2\rho$ of the electron density $\rho(\mathbf{r})$ and also other related quantities at the bond critical points with the objective of rationalizing the relative stability of the two isomers in both $(H_2O)_2^+$ and $(H_2S)_2^+$.

## 1. Introduction

In recent years, density functional theory[1] (DFT) has emerged as one of the most powerful theoretical tools not only for a quantitative prediction of the electronic structure and properties of atoms, molecules, and solids but also for a rigorous foundation to many widely used chemical concepts.[2−5] One great advantage of DFT is that the electron correlation effect is taken into account here at a much less computational cost and the predicted quantitative results are comparable to those obtained from various post-Hartree−Fock (HF) methods involving extensive computer time. However, one major drawback in the practical implementation of DFT is that the "exact" form of the exchange−correlation (XC) energy density functional is not known for an inhomogeneous electron density distribution as present in atomic or molecular systems. For the homogeneous electron gas, however, a suitable expression for the XC functional is known and it forms the basis of the so-called local density approximation (LDA) corresponding to a locally homogeneous approximation for an otherwise inhomogeneous density distribution. However, because of poor performance of LDA in predicting molecular properties, several other modified XC energy density fuctionals have been proposed from time to time. Most of these functionals involve gradient corrections in some form or the other, and few of them have been in use for more than a decade with good performance. A crucial test of an XC functional, however, depends on its predictive ability in difficult or controversial situations. One such system of current interest has been the singly ionized water dimer for which the nature of the bond between the two water molecules and hence the structure of the ionized dimer[6−11] have been controversial. The ionized hydrogen-bonded systems such as this have been known to exhibit a rich and varied chemistry due to the associated processes such as proton transfer and molecular rearrangements. Although theoretical studies on neutral water dimer formed by a hydrogen bond have been quite extensive, investigations on the electronic and molecular structures of the corresponding radical cations have been much less.[11]

Understanding the nature of a hydrogen bond has been the subject of increasing research activities[12−15] in recent years due to its importance in many chemical and biological systems and processes, as well as in the crystal packing of many organic and organometallic compounds. Even the nature of interactions involved in an O−H···O hydrogen bond sometimes appears to be controversial.[16−17] The structures of neutral water dimer and the two isomers of its cation as obtained on ionization are shown in Figure 1. For this system, calculations based on the post-HF methods predict the proton-transferred $(HO-H_3O)^+$ isomer to be the ground state and this structure is found[6] to be about 8.9 kcal/mol lower in energy than the corresponding hemi-bonded $(H_2O-OH_2)$ isomer at the MP4 level of theory, which is also confirmed by the modified coupled pair functional method.[7] The recent density functional calculations[8−10] with a few gradient-corrected XC functionals (such as BP86, BLYP, B3LYP, etc.), however, predict the hemi-bonded isomer as the minimum energy structure, while the same with 50% exact HF exchange (in BHHLYP functional) does not show any discrepancy and predicts[10] the $(HO-H_3O)^+$ proton-transferred isomer to be lower in energy. For an analogous system, namely, $(H_2S)_2^+$, however, both post-HF and DFT calculations are found to lead to an identical conclusion[18,19] predicting the hemi-bonded structure as the lower energy one. It is thus clear that the DFT-predicted

* To whom correspondence should be addressed. T.K.G.: E-mail: tapang@apsara.barc.ernet.in. S.K.G.: E-mail: skghosh@magnum.barc.ernet.in.

10.1021/jp0264275 CCC: $22.00 
Published on Web 11/12/2002

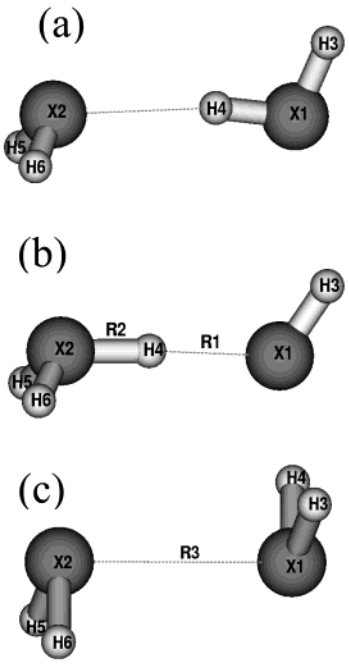


**Figure 1.** Structures of (a) neutral, (b) proton-transferred cation, and (c) hemi-bonded cation (X = O for $(H_2O)_2$ and $(H_2O)_2^+$, and X = S for $(H_2S)_2$ and $(H_2S)_2^+$).

result depends heavily on the nature of the XC functional used, and recently, Sodupe et al.[10] have ascribed this discrepancy for $(H_2O)_2^+$ to an overestimation of the XC energy functional due to the self-interaction error. In view of this discrepancy between the post-HF predictions and the density functional results for the ground state structure of this system and the importance of understanding the structure of ionized hydrogen-bonded systems, it would be of interest to carry out a detailed density functional investigation on these systems and to understand the origin of the discrepancy particularly because the density functionals have been known to lead to successful prediction in most of the cases including some of the loosely bound transition states. Moreover, for the $(H_2S)_2^+$ system, no systematic study has been reported using either the DFT or the complete active space self-consistent field (CASSCF) methods. Thus, we propose to study the multiconfiguration effect on the structures of different isomers and energetics for $(H_2O)_2^+$ and $(H_2S)_2^+$ open-shell radical systems by employing CASSCF theory to determine the ground state isomer of water dimer radical cation as well as hydrogen sulfide dimer radical cation and to calculate the accurate energy difference between the two isomers using the CASSCF wave function followed by multireference perturbation treatment, which has been successful[20] for many complicated systems where conventional DFT has failed to predict correct results.

In this work, our objective is to assess the performance of different XC energy density functionals in the DFT framework for predicting the minimum energy structures of $(H_2O)_2^+$ and $(H_2S)_2^+$, particularly in view of the recently created controversy between DFT and post-HF methods for $(H_2O)_2^+$. The performance of various XC functionals in the DFT framework for predicting the dissociation energy of a number of systems has recently been studied independently by Braïda et al.[21] and Grüning et al.[22] assuming the hemi-bonded structures involving two center−three electron (2c−3e) bonds. However, our aim here is to assess the performance of different XC functionals in predicting the energy difference of the two isomers, namely, the proton-transferred structure and hemi-bonded species in $(H_2O)_2^+$ and $(H_2S)_2^+$, and also to see if there exists any trend between the total energy difference and the XC energy difference (for various functionals) of the two isomers.

Besides the energetic considerations, another tool that has been quite valuable in providing insight into the structure and bonding in molecules involves the topological analysis[23,24] of the electron density $\rho(\mathbf{r})$, which has proved to be highly successful in the prediction and rationalization of various aspects of chemical binding and reactivity. Recently, this approach has been extensively used[25−28] for studies of interesting and unusual bonding aspects in molecular systems. The studies reported so far on $(H_2O)_2^+$ and $(H_2S)_2^+$ have however dealt with mainly the total energy quantities, and the information provided by the topological features of the electron density $\rho(\mathbf{r})$ has not been utilized. A study of the geometry change of the water dimer on ionization has been reported[11] recently through an in-depth analysis of the associated energy barriers as well as variation of different chemical reactivity indices such as hardness, electronegativity, and polarizability during the proton transfer process. A still better understanding of the interactions underlying the relative stabilities can be achieved through detailed studies on the topological aspects of the electron distribution of the isomers. We thus propose to employ the topological theory of atoms in molecules (AIM),[23−24] which has been known to provide a rigorous procedure to partition a molecular system into its atomic fragments defined by the gradient vector field $\nabla\rho(\mathbf{r})$ and provide thereby an unambiguous definition of chemical bonding through the bond path and bond critical point (BCP) properties. The AIM framework makes a bridge between the quantitative results obtained from quantum chemical calculations and the traditional chemical concepts. The study presented here is thus intended not only to investigate the multiconfigurational effect and to explore the assessment of the XC functionals in predicting the relative energy of the isomers but also to analyze the electron density distribution as obtained using various XC functionals for different bonding situations present in the two isomers of $(H_2O)_2^+$ and $(H_2S)_2^+$.

The plan of the paper is as follows. We discuss the computational method in Section 2 and the results of numerical calculations in Section 3. Finally, we present the concluding remarks in Section 4.

## 2. Computational Methods

Ab initio molecular orbital methods have been used here to investigate the structures of the two most stable isomers of $(H_2O)_2^+$ and $(H_2S)_2^+$ radical systems. The geometries of the two isomers have been fully optimized with the CASSCF method in which the active space includes all of the valence electrons and all of the valence orbitals except the oxygen 2s orbitals. This results in an active space of 11 electrons and 10 orbitals, which is referred to as CAS(11/10). Single point second-order multiconfigurational quasi-degenerate perturbation theory (MCQDPT2)[29] calculations have been carried out at the CAS(11/10) optimized geometries in order to improve the energies. Density functional calculations using several XC energy density functionals have also been performed to optimize the geometry of the two isomers of $(H_2O)_2^+$ and $(H_2S)_2^+$. The ab initio calculations in this work have been performed using the GAMESS[30] electronic structure program using three basis sets, namely, 6-31++G(d,p), 6-31++G(2d,p), and 6-31++G-(2d,2p). The different exchange energy density functionals considered in this work are due to Slater,[31] Becke,[32] Gill,[33] and Perdew−Burke−Ernzerhof (PBE),[34] while the correlation energy density functionals used are due to Vosko−Wilk−Nusair (VWN),[35] Lee−Yang−Parr (LYP),[36] and also one parameter

**TABLE 1: Calculated Relative Total Energies ($\Delta E$)[a] and XC Energies ($\Delta E_{XC}$)[a] for the Two Isomers of $(H_2O)_2^+$ Using Different Methods and Basis Sets**

| | 6-31++G(d,p) | | 6-31++G(2d,p) | | 6-31++G(2d,2p) | |
|---|---|---|---|---|---|---|
| method[b] | $\Delta E$ | $\Delta E_{XC}$ | $\Delta E$ | $\Delta E_{XC}$ | $\Delta E$ | $\Delta E_{XC}$ |
| SLATER | 8.0 | −12.3 | 8.8 | −10.9 | 8.8 | −11.0 |
| SVWN | 10.0 | −9.8 | 10.9 | −8.3 | 10.9 | −8.4 |
| SLYP | 10.8 | −7.9 | 11.7 | −6.4 | 11.7 | −6.5 |
| SOP | 9.6 | −10.3 | 10.4 | −9.0 | 10.3 | −9.1 |
| BECKE | 6.3 | −16.6 | 6.9 | −15.9 | 6.9 | −16.0 |
| BVWN | 8.2 | −14.7 | 8.8 | −13.7 | 8.7 | −13.8 |
| BLYP | 8.4 | −13.8 | 9.0 | −12.7 | 9.0 | −12.7 |
| BOP | 8.9 | −13.2 | 9.5 | −12.2 | 9.5 | −12.4 |
| GILL | 5.8 | −17.3 | 6.3 | −16.5 | 6.3 | −16.7 |
| GVWN | 7.6 | −15.5 | 8.2 | −14.3 | 8.2 | −14.6 |
| GLYP | 7.8 | −14.4 | 8.4 | −13.4 | 8.4 | −13.5 |
| PBE | 7.0 | −15.9 | 7.5 | −15.0 | 7.5 | −15.2 |
| PBEVWN | 8.88 | −13.9 | 9.4 | −12.9 | 9.4 | −13.0 |
| PBELYP | 9.1 | −12.9 | 9.7 | −11.8 | 9.8 | −11.8 |
| PBEOP | 9.5 | −12.5 | 10.1 | −11.4 | 10.1 | −11.5 |
| ROHF | −33.0 | | −32.0 | | −32.3 | |
| UHF | −27.4 | | −26.2 | | −26.5 | |
| HLYP | −23.5 | 3.9 | −22.3 | 4.0 | −22.5 | −4.0 |
| HOP | −23.5 | 3.9 | −22.4 | 3.9 | −22.7 | 3.9 |
| B3LYP | 1.0 | −10.4 | 1.8 | −9.5 | 1.7 | −9.5 |
| BHHLYP | −9.2 | −5.2 | −8.3 | −4.7 | −8.4 | −4.6 |
| CASSCF | −21.2 | | −20.5 | | −20.8 | |
| MCQDPT2 | −3.2 | | −1.4 | | −1.9 | |

[a] The energy difference $\Delta E = E$(proton-transferred) − $E$(hemi-bonded) and $\Delta E_{XC} = E_{XC}$(proton-transferred) − $E_{XC}$(hemi-bonded), where $E$ is the total energy and $E_{XC}$ is the XC energy component. [b] The symbols are the same as used in GAMESS program and correspond to different combinations of the XC functionals. Each exchange only functional corresponding to Slater, Becke, Gill, PBE, and HF are followed here by combinations with the correlation functionals VWN, LYP, and OP.

progressive functional (OP) proposed by Tsuneda et al.[37] Various possible combinations of exchange and correlation functionals are considered for performing the DFT calculations. Apart from these, the full HF exchange along with DFT correlation (e.g., HLYP, HOP) as well as hybrid functionals involving a fractional amount of HF exchange and LYP correlation, namely, Becke half and half functional (BHHLYP)[38] and three parameter Becke exchange along with LYP correlation (B3LYP),[39] have also been studied. The topological properties of the electronic charge density have been calculated using the program AIMPAC.[40]

### 3. Results and Discussion

The two lower energy stationary structures of $(H_2O)_2^+$ and $(H_2S)_2^+$ that can be obtained on ionization of the neutral species are presented in Figure 1. The lowest electronic state for the three electron hemi-bonded structure has been found to be $^2B_u$ while the same for the proton-transferred structure is $^2A''$, which has already been observed by earlier workers. The total energy differences based on unrestricted DFT as well as other methods and also the XC energy differences between the two structures of $(H_2O)_2^+$ are reported in Table 1 from which it is evident that the hemi-bonded isomer is more stable than the proton-transferred one for all of the XC energy density functionals except a very few like the BHHLYP functional and full HF exchange with local correlation functionals (e.g., HLYP and HOP). The self-consistently calculated relative XC energy values are, however, lower for the proton-transferred structure, which is contrary to the trend in the relative total energy values using DFT as mentioned above. This is contrary to the expectations in the light of the recent analysis as done by Grüning et al.[22] They have ascribed the overestimation of the stability of the hemi-bonded structure as the absence of left−right correlation in this type of system. It is also to be noted that with increase in the size of the basis set, the energy difference is converged. From the table, it is clear that the more sophisticated methods such as CASCF and CASCSF+MCQDPT2 predict the proton-transferred structure to be more stable as compared to the three electron hemi-bonded structure, which is consistent with the previous results obtained using MP2 and CCSD(T) levels of theory. The CASSCF method, however, slightly overestimates the energy difference whereas the CASCSF+MCQDPT2 method underestimates it slightly in comparison to the MP2 and CCSD(T) predicted values (5.2 and 6.6 kcal/mol, respectively). Because the electron correlation is known[41] to be dynamic in odd electron bonding (2c−3e bonds), it is clear that the CASSCF method (having no provision for dynamic electron correlation effect) has not performed well here. In this context, it is to be noted that the failure of the CASSCF method in the bond dissociation of hydrogen peroxide and its anion had earlier been reported[42] by Benassi and Taddei. Thus, it is clear that the electron correlation due to the multiconfiguration effect is stronger in the hemi-bonded structure in comparison to the proton-transferred one. Nevertheless, the XC functionals without any fraction of the HF exchange cannot reproduce the relative stability of the $(H_2O)_2^+$ isomers in agreement with the post-HF predictions. It is also to be noted that the calculated energy difference using full HF exchange with local correlation (−22.5 kcal/mol in HLYP and −22.7 kcal/mol in HOP) deviates more from the MCQDPT2 result (−1.9 kcal/mol) than the result (−8.4 kcal/mol) obtained using the half and half exchange with local correlation. In fact, among all of the XC density functionals studied here, the performance of the B3LYP functional is the best if one considers the smallest percentage deviation from the MCQDPT2 calculated result, although the former predicts the hemi-bonded isomer to be more stable. Both ROHF and UHF methods are found to underestimate the stability of the hemi-bonded structure in comparison to the DFT methods. It is also evident from the fact that the calculated results with various XC functionals using the CASSCF/6-31G++(2d,2p) optimized geometries are almost the same as obtained by using the individually optimized geometries with various XC energy functionals. Thus, apart from the effect on the geometry, different XC functionals have a considerable effect on the single point energies for both of the isomers. It is also to be noted that the effect of dynamic electron correlation through MCQDPT2 calculations on the relative energy of the $(H_2O)_2^+$ isomers is very significant, with corrections up to 19 kcal/mol (see Table 1).

The calculated values of the total energy differences and the XC energy differences for the $(H_2S)_2^+$ ion are presented in Table 2, and the results indicate that the hemi-bonded isomer is more stable irrespective of the method of calculation, although the relative energy differences vary from one method to another. Here, the calculated total energy differences and the corresponding XC energy differences show the same trend as far as the relative stability of the isomers is concerned. It is to be noted that the results obtained using different XC functionals are fairly constant except those obtained using HOP and HLYP functionals. The performance of the full HF exchange with local correlation as in HLYP and HOP is very good, and the respective relative energy values of 10.1 and 10.0 kcal/mol compare very well with the same (8.0 kcal/mol) obtained from MCQDPT2 calculation. Unlike in the case of the $(H_2O)_2^+$ system, the effect of dynamic electron correlation on the relative

**TABLE 2: Calculated Relative Total Energies ($\Delta E$)[a] and XC Energies ($\Delta E_{XC}$)[a] for the Two Isomers of $(H_2S)_2^+$ Using Different Methods and Basis Sets**

| | 6-31++G(d,p) | | 6-31++G(2d,p) | | 6-31++G(2d,2p) | |
|---|---|---|---|---|---|---|
| method | $\Delta E$ | $\Delta E_{XC}$ | $\Delta E$ | $\Delta E_{XC}$ | $\Delta E$ | $\Delta E_{XC}$ |
| SLATER | 15.2 | 0.9 | 16.2 | 3.4 | 16.1 | 3.6 |
| SVWN | 17.7 | 4.5 | 19.0 | 7.6 | 18.8 | 7.9 |
| SLYP | 17.9 | 6.0 | 19.3 | 9.2 | 19.2 | 9.5 |
| SOP | 17.0 | 3.5 | 18.2 | 6.4 | 18.1 | 6.6 |
| BECKE | 16.0 | −0.2 | 16.3 | 1.1 | 16.3 | 1.0 |
| BVWN | 18.2 | 2.6 | 18.7 | 4.3 | 18.6 | 4.3 |
| BLYP | 17.9 | 2.7 | 18.5 | 4.6 | 18.4 | 4.6 |
| BOP | 18.4 | 3.1 | 18.9 | 5.0 | 18.8 | 5.1 |
| GILL | 15.7 | −0.6 | 16.0 | 0.7 | 15.9 | 0.6 |
| GVWN | 17.8 | 2.0 | 18.3 | 3.9 | 18.3 | 4.0 |
| GLYP | 17.4 | 2.2 | 18.1 | 4.2 | 18.0 | 4.2 |
| PBE | 16.2 | 0.1 | 16.5 | 1.4 | 16.5 | 1.3 |
| PBEVWN | 18.4 | 2.9 | 18.9 | 4.5 | 18.8 | 4.6 |
| PBELYP | 18.1 | 3.2 | 18.7 | 4.7 | 18.6 | 4.9 |
| PBEOP | 18.5 | 3.5 | 19.1 | 5.3 | 19.0 | 5.3 |
| ROHF | 2.0 | | 3.2 | | 3.1 | |
| UHF | 4.1 | | 5.4 | | 5.3 | |
| HLYP | 8.5 | 4.4 | 10.3 | 4.9 | 10.1 | 4.8 |
| HOP | 8.4 | 4.3 | 10.2 | 4.8 | 10.0 | 4.8 |
| B3LYP | 16.2 | 3.2 | 17.0 | 4.9 | 16.9 | 5.0 |
| BHHLYP | 13.4 | 3.7 | 14.6 | 5.0 | 14.5 | 5.0 |
| CASSCF | 7.8 | | 4.0 | | 3.9 | |
| MCQDPT2 | 12.7 | | 7.9 | | 8.0 | |

[a] The energy difference $\Delta E = E$(proton-transferred) $- E$(hemi-bonded) and $\Delta E_{XC} = E_{XC}$(proton-transferred) $- E_{XC}$(hemi-bonded), where $E$ is the total energy and $E_{XC}$ is the XC energy component.

energy of the $(H_2S)_2^+$ isomers is not very significant, with corrections only up to 4 kcal/mol (see Table 2).

It will now be of interest to analyze the nature of interactions involved in the $(H_2O)_2^+$ and $(H_2S)_2^+$ systems within the framework of Bader's topological theory of AIM.[23,24] A BCP (point corresponding to $\nabla\rho = 0$) is found between each pair of nuclei, which are considered to be linked by a chemical bond, with two negative curvatures ($\lambda_1$ and $\lambda_2$) and one positive curvature ($\lambda_3$) denoted as the (3,−1) critical point. The bond ellipticity ($\epsilon$) defined in terms of the two negative curvatures as $\epsilon = (\lambda_1/\lambda_2 - 1)$ reflects the deviation of the charge distribution of a bond path from axial symmetry, thus providing a sensitive measure of the susceptibility of a system to undergo a structural change. The Lapalacian of the electronic charge density ($\nabla^2\rho$) indicates whether the electron density is locally concentrated ($\nabla^2\rho < 0$) or depleted ($\nabla^2\rho > 0$) and provides a detailed map of the basic and acidic regions of a molecule. The plots of $\nabla^2\rho$ for the proton-transferred (Figure 2) as well as hemi-bonded (Figure 3) structures of $(H_2O)_2^+$ presented here are shown to reveal these gross features quite well. Both Figures 2 and 3 reflect the "closed-shell" type interaction between the two weakly bonded fragments involving the O1···H4 bond in $(HO\cdots H_3O)^+$ and the O1···O2 bond in $(H_2O\cdots OH_2)^+$. A better quantitative comparison of the nature of bonding should follow from the values of this quantity at the BCP and also from the other BCP properties. Thus, a value of $\nabla^2\rho < 0$ at a BCP is unambiguously related to the covalent character of a bond, indicating a sharing of electrons and referred to as a "shared" type interaction, while $\nabla^2\rho > 0$ implies a closed-shell type interaction as found in noble gas repulsive states, ionic bonds, hydrogen bonds, and van der Waals molecules. Bader has also defined a local electronic energy density ($E_d(r)$) as $E_d(r) = G(r) + V(r)$, where $G(r)$ and $V(r)$ correspond to local kinetic and potential energy densities, respectively. The sign of $E_d(r)$ determines whether accumulation of charge at a given point $r$ is stabilizing ($E_d(r) < 0$) or destabilizing ($E_d(r) > 0$).

Thus, the calculated values of the electron density ($\rho$), Laplacian ($\nabla^2\rho$), bond ellipticity ($\epsilon$), and electronic energy density ($E_d$) at the BCP for the weakest bond (X1···H4) in proton-transferred and (X1···X2) in hemi-bonded isomers of $(H_2X)_2^+$ (X = O, S) are presented in Tables 3 and 4, respectively. The DFT results on the electron density for the O1···H4 bond at the BCP in the proton-transferred structure are higher as compared to the corresponding HF results, and the same trend is also reflected in the case of the S1···H4 bond indicating the DFT-predicted bond strengths of both these bonds to be stronger than the HF-predicted ones. The calculated values of the other properties at the BCP, namely, the Laplacian of the electron density, the bond ellipticity, and the local electronic energy density, also follow the same trend. On the other hand, the BCP electron density values calculated using DFT for the O1···O2 and S1···S2 bonds in the hemi-bonded structure are found to be smaller than the corresponding HF results.

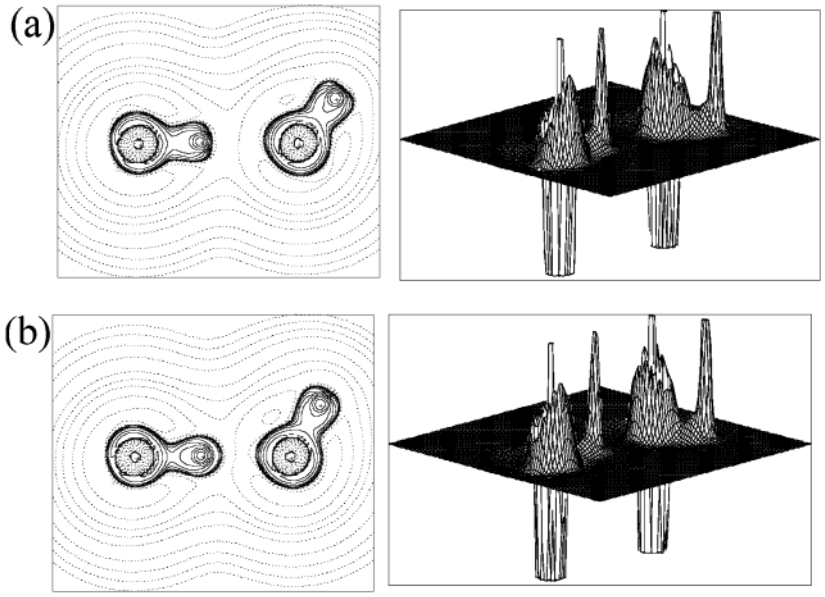


**Figure 2.** Contour plots and relief maps of $\nabla^2\rho$ for the proton-transferred structure of $(H_2O)_2^+$: (a) HF calculations and (b) DFT calculations using the B3LYP XC functional.

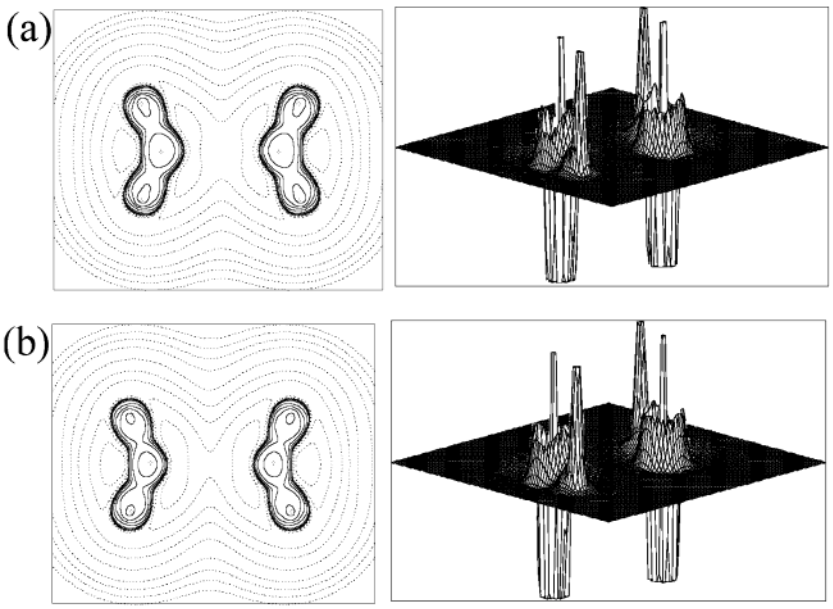


**Figure 3.** Contour plots and relief maps of $\nabla^2\rho$ for the hemi-bonded structure of $(H_2O)_2^+$: (a) HF calculations and (b) DFT calculations using the B3LYP XC functional.

**TABLE 3: Calculated Values of BCP Properties of the O1···H4 Bond in $(HO\cdots H_3O)^+$ and the O1···O2 Bond in $(H_2O\cdots OH_2)^+$ Radical Cations Using Different Methods**

| method | R1[a] (Å) | $\rho$ (au) | $\nabla^2\rho$ (au) | $\epsilon$ | $E_d(r)$ (au) | R3[a] (Å) | $\rho$ (au) | $\nabla^2\rho$ (au) | $\epsilon$ | $E_d(r)$ (au) |
|---|---|---|---|---|---|---|---|---|---|---|
| SLATER | 1.380 | 0.107 | 0.005 | 0.021 | −0.059 | 2.133 | 0.051 | 0.214 | 0.048 | 0.009 |
| SVWN | 1.350 | 0.116 | −0.027 | 0.021 | −0.073 | 2.087 | 0.056 | 0.246 | 0.048 | 0.009 |
| SLYP | 1.333 | 0.121 | −0.063 | 0.022 | −0.084 | 2.056 | 0.061 | 0.268 | 0.046 | 0.009 |
| SOP | 1.360 | 0.113 | −0.016 | 0.021 | −0.068 | 2.103 | 0.054 | 0.234 | 0.048 | 0.009 |
| BECKE | 1.521 | 0.073 | 0.115 | 0.021 | −0.016 | 2.319 | 0.033 | 0.121 | 0.056 | 0.006 |
| BVWN | 1.479 | 0.082 | 0.116 | 0.022 | −0.023 | 2.256 | 0.037 | 0.149 | 0.055 | 0.008 |
| BLYP | 1.441 | 0.091 | 0.093 | 0.022 | −0.032 | 2.205 | 0.042 | 0.174 | 0.053 | 0.009 |
| BOP | 1.455 | 0.088 | 0.099 | 0.021 | −0.029 | 2.232 | 0.040 | 0.160 | 0.054 | 0.008 |
| GILL | 1.511 | 0.076 | 0.111 | 0.021 | −0.019 | 2.322 | 0.033 | 0.120 | 0.056 | 0.006 |
| GVWN | 1.470 | 0.084 | 0.110 | 0.021 | −0.025 | 2.258 | 0.037 | 0.148 | 0.055 | 0.008 |
| GLYP | 1.433 | 0.093 | 0.085 | 0.021 | −0.036 | 2.204 | 0.042 | 0.174 | 0.053 | 0.009 |
| PBE | 1.511 | 0.075 | 0.114 | 0.022 | −0.018 | 2.303 | 0.034 | 0.128 | 0.056 | 0.007 |
| PBEVWN | 1.474 | 0.083 | 0.116 | 0.022 | −0.023 | 2.242 | 0.038 | 0.156 | 0.055 | 0.008 |
| PBELYP | 1.438 | 0.091 | 0.092 | 0.022 | −0.033 | 2.195 | 0.043 | 0.180 | 0.052 | 0.009 |
| PBEOP | 1.452 | 0.088 | 0.098 | 0.021 | −0.030 | 2.221 | 0.041 | 0.166 | 0.053 | 0.009 |
| ROHF | 1.579 | 0.054 | 0.163 | 0.043 | −0.005 | 1.992 | 0.073 | 0.309 | 0.058 | 0.005 |
| UHF | 1.578 | 0.054 | 0.163 | 0.043 | −0.005 | 2.022 | 0.069 | 0.284 | 0.056 | 0.006 |
| HLYP | 1.485 | 0.070 | 0.174 | 0.039 | −0.016 | 1.966 | 0.078 | 0.330 | 0.056 | 0.004 |
| HOP | 1.507 | 0.066 | 0.175 | 0.039 | −0.013 | 1.974 | 0.076 | 0.324 | 0.056 | 0.004 |
| B3LYP | 1.447 | 0.086 | 0.108 | 0.030 | −0.029 | 2.128 | 0.051 | 0.218 | 0.053 | 0.009 |
| BHHLYP | 1.470 | 0.077 | 0.139 | 0.034 | −0.022 | 2.054 | 0.061 | 0.266 | 0.054 | 0.009 |

[a] R1 is the bond length of the O1···H4 bond in $(HO\cdots H_3O)^+$, and R3 is the bond length of the O1···O2 bond in $(H_2O\cdots OH_2)^+$ (see Figure 1).

It is thus clear that the relative stability of the two isomers as determined from the total energy difference as reported in Tables 1 and 2, which reveal that the hemi-bonded isomer containing the O1···O2 bond is more stable in DFT in comparison to the HF theory, cannot be rationalized by considering alone the BCP properties of the weakest bonds in the $(H_2O)_2^+$ isomers, namely, O1···H4 and O1···O2 bonds, and perhaps consideration of the next weaker bond might throw light in rationalizing the underestimation of the stability of the proton-transferred structure of the $(H_2O)_2^+$ ion. In view of this, we have also analyzed the electron density distribution of the O2−H4 bond and S2−H4 bonds in $(H_2O)_2^+$ and $(H_2S)_2^+$ ions, respectively, and the relevant BCP properties reported in Table 5 reveal that both of these bonds are highly covalent in nature as demonstrated by large and negative values of the Laplacian for all of the reported methods and can be considered as normal covalent bonds. However, it is also important here to compare the relative values of the electron density and other properties as obtained by different methods. The HF values of the electron density at the BCP in this bond are much higher in comparison to the same calculated using DFT methods, which is consistent with a lower stability of the proton-transferred isomer predicted by the DFT methods. Similarly, a higher value of this bond length predicted by DFT as reported in Table 5 is also indicative of the same trend. Because the O2−H4 bond is much stronger than the O1···H4 bond in $(HO\cdots H_3O)^+$ or the O1···O2 bond in $(H_2O\cdots OH_2)^+$, the strength of this bond is likely to play a more dominating role in determining the relative stability of the isomers, and this is one of the reasons for the lower stability of the proton-transferred structure in comparison to the hemi-bonded one. Thus, it is clear that the geometry relaxation effect is likely to play a significant role in the overestimation[20] of the bond dissociation energy of the hemi-bonded structure as predicted by DFT-based methods.

Besides the Bader's topological theory of AIM, an interesting alternative approach due originally to Silvi and Savin[43] can also

**TABLE 4: Calculated Values of BCP Properties of the S1···H4 Bond in $(HS\cdots H_3S)^+$ and the S1···S2 Bond in $(H_2S\cdots SH_2)^+$ Radical Cations Using Different Methods**

| | S1···H4 | | | | | S1···S2 | | | | |
|---|---|---|---|---|---|---|---|---|---|---|
| method | R1[a] (Å) | $\rho$ (au) | $\nabla^2\rho$ (au) | $\epsilon$ | $E_d(r)$ (au) | R3[a] (Å) | $\rho$ (au) | $\nabla^2\rho$ (au) | $\epsilon$ | $E_d(r)$ (au) |
| SLATER | 1.781 | 0.090 | −0.049 | 0.001 | −0.034 | 2.871 | 0.035 | 0.050 | 0.034 | −0.003 |
| SVWN | 1.743 | 0.097 | −0.058 | 0.000 | −0.039 | 2.791 | 0.040 | 0.055 | 0.035 | −0.005 |
| SLYP | 1.733 | 0.098 | −0.063 | 0.002 | −0.040 | 2.751 | 0.043 | 0.057 | 0.034 | −0.006 |
| SOP | 1.755 | 0.095 | −0.056 | 0.000 | −0.037 | 2.816 | 0.038 | 0.053 | 0.035 | −0.004 |
| BECKE | 1.980 | 0.061 | 0.005 | 0.007 | −0.017 | 3.165 | 0.020 | 0.036 | 0.035 | 0.001 |
| BVWN | 1.909 | 0.053 | 0.029 | 0.110 | −0.013 | 3.051 | 0.024 | 0.043 | 0.036 | 0.000 |
| BLYP | 1.849 | 0.079 | −0.020 | 0.005 | −0.026 | 2.985 | 0.028 | 0.046 | 0.035 | −0.001 |
| BOP | 1.863 | 0.078 | −0.017 | 0.005 | −0.026 | 3.009 | 0.027 | 0.045 | 0.036 | −0.001 |
| GILL | 1.954 | 0.064 | 0.000 | 0.006 | −0.019 | 3.164 | 0.020 | 0.036 | 0.035 | 0.001 |
| GVWN | 1.887 | 0.056 | 0.026 | 0.109 | −0.014 | 3.048 | 0.025 | 0.043 | 0.036 | 0.000 |
| GLYP | 1.833 | 0.082 | −0.025 | 0.004 | −0.028 | 2.979 | 0.028 | 0.046 | 0.036 | −0.001 |
| PBE | 1.969 | 0.062 | 0.004 | 0.006 | −0.018 | 3.139 | 0.021 | 0.037 | 0.034 | 0.001 |
| PBEVWN | 1.899 | 0.054 | 0.028 | 0.109 | −0.013 | 3.030 | 0.025 | 0.044 | 0.035 | 0.000 |
| PBELYP | 1.843 | 0.080 | −0.021 | 0.004 | −0.027 | 2.969 | 0.029 | 0.047 | 0.035 | −0.001 |
| PBEOP | 1.855 | 0.079 | −0.019 | 0.005 | −0.026 | 2.992 | 0.027 | 0.045 | 0.035 | −0.001 |
| ROHF | 2.403 | 0.021 | 0.039 | 0.010 | −0.001 | 2.804 | 0.041 | 0.051 | 0.052 | −0.006 |
| UHF | 2.399 | 0.021 | 0.040 | 0.010 | −0.001 | 2.819 | 0.040 | 0.050 | 0.050 | −0.005 |
| HLYP | 2.219 | 0.031 | 0.046 | 0.009 | −0.004 | 2.728 | 0.046 | 0.054 | 0.050 | −0.008 |
| HOP | 2.253 | 0.029 | 0.045 | 0.010 | −0.003 | 2.735 | 0.046 | 0.054 | 0.051 | −0.008 |
| B3LYP | 1.907 | 0.065 | 0.017 | 0.004 | −0.018 | 2.899 | 0.033 | 0.049 | 0.039 | −0.002 |
| BHHLYP | 2.061 | 0.046 | 0.037 | 0.007 | −0.009 | 2.823 | 0.038 | 0.052 | 0.044 | −0.004 |

[a] R1 is the bond length of the S1···H4 bond in $(HS\cdots H_3S)^+$, and R3 is the bond length of the S1···S2 bond in $(H_2S\cdots SH_2)^+$ (see Figure 1).

**TABLE 5: Calculated Values of Bond Distance (R2)[a] and BCP Properties of the O2−H4 Bond in $(HO\cdots H_3O)^+$ and the S2−H4 Bond in $(HS\cdots H_3S)^+$ Radical Cations Using Different Methods**

| | $(H_2O)_2^+$ | | | | | $(H_2S)_2^+$ | | | | |
|---|---|---|---|---|---|---|---|---|---|---|
| method | R2 (Å) | $\rho$ (au) | $\nabla^2\rho$ (au) | $\epsilon$ | $E_d(r)$ (au) | R2 (Å) | $\rho$ (au) | $\nabla^2\rho$ (au) | $\epsilon$ | $E_d(r)$ (au) |
| SLATER | 1.132 | 0.211 | −0.894 | 0.021 | −0.295 | 1.648 | 0.110 | −0.072 | 0.016 | −0.049 |
| SVWN | 1.117 | 0.219 | −0.926 | 0.021 | −0.310 | 1.620 | 0.117 | −0.081 | 0.016 | −0.055 |
| SLYP | 1.125 | 0.212 | −0.862 | 0.021 | −0.295 | 1.628 | 0.114 | −0.073 | 0.015 | −0.053 |
| SOP | 1.123 | 0.216 | −0.911 | 0.021 | −0.304 | 1.631 | 0.114 | −0.077 | 0.016 | −0.053 |
| BECKE | 1.091 | 0.249 | −1.248 | 0.020 | −0.374 | 1.566 | 0.138 | −0.163 | 0.020 | −0.070 |
| BVWN | 1.079 | 0.257 | −1.293 | 0.020 | −0.392 | 1.553 | 0.136 | −0.171 | 0.023 | −0.067 |
| BLYP | 1.094 | 0.243 | −1.167 | 0.020 | −0.362 | 1.587 | 0.130 | −0.124 | 0.019 | −0.064 |
| BOP | 1.090 | 0.247 | −1.202 | 0.020 | −0.370 | 1.579 | 0.133 | −0.134 | 0.019 | −0.067 |
| GILL | 1.093 | 0.247 | −1.227 | 0.020 | −0.370 | 1.576 | 0.135 | −0.151 | 0.020 | −0.068 |
| GVWN | 1.081 | 0.255 | −1.271 | 0.020 | −0.387 | 1.562 | 0.132 | −0.159 | 0.023 | −0.064 |
| GLYP | 1.096 | 0.241 | −1.146 | 0.021 | −0.358 | 1.594 | 0.128 | −0.116 | 0.019 | −0.062 |
| PBE | 1.093 | 0.247 | −1.230 | 0.020 | −0.370 | 1.569 | 0.137 | −0.160 | 0.019 | −0.069 |
| PBEVWN | 1.079 | 0.256 | −1.286 | 0.020 | −0.390 | 1.557 | 0.134 | −0.166 | 0.023 | −0.066 |
| PBELYP | 1.094 | 0.242 | −1.163 | 0.020 | −0.361 | 1.589 | 0.129 | −0.122 | 0.018 | −0.064 |
| PBEOP | 1.091 | 0.246 | −1.193 | 0.020 | −0.368 | 1.583 | 0.132 | −0.130 | 0.019 | −0.066 |
| ROHF | 1.002 | 0.306 | −2.436 | 0.018 | −0.664 | 1.367 | 0.216 | −0.594 | 0.036 | −0.176 |
| UHF | 1.003 | 0.305 | −2.423 | 0.018 | −0.661 | 1.367 | 0.216 | −0.592 | 0.036 | −0.175 |
| HLYP | 1.008 | 0.295 | −2.305 | 0.018 | −0.639 | 1.372 | 0.213 | −0.592 | 0.033 | −0.175 |
| HOP | 1.004 | 0.301 | −2.389 | 0.018 | −0.659 | 1.367 | 0.216 | −0.604 | 0.034 | −0.179 |
| B3LYP | 1.070 | 0.253 | −1.309 | 0.020 | −0.397 | 1.527 | 0.148 | −0.225 | 0.022 | −0.085 |
| BHHLYP | 1.040 | 0.273 | −1.650 | 0.019 | −0.479 | 1.439 | 0.181 | −0.399 | 0.026 | −0.128 |

[a] See Figure 1.

be used through consideration of the electron localization function. In an interesting recent work, Fourré et al.[44] have presented a topological characteristic of the three electron-bonded radical ions.

## 4. Concluding Remarks

The performance of the different XC energy density functionals has been assessed here in predicting the relative stability of the $(H_2O)_2^+$ and $(H_2S)_2^+$ isomers with reference to the CASSCF and MCQDPT2 calculated results. In the case of the $(H_2O)_2^+$ system, XC functionals with full HF exchange and local correlation or half and half exchange and local correlation predict the relative stability of the proton-transferred structure correctly. However, the performance of the B3LYP functional is found to be the best in terms of absolute deviation in the energy difference from the corresponding MCQDPT2 value. The performance of the functionals with full HF exchange and local correlation (as in HLYP and HOP) is very good in the case of $(H_2S)_2^+$ isomers. The calculated values of the XC energy component do not show any regular trend with that of the total energy difference for both $(H_2O)_2^+$ or $(H_2S)_2^+$. Dynamical electron correlation effect calculated using the MCQDPT2 method is found to be much stronger in $(H_2O)_2^+$ as compared to $(H_2S)_2^+$.

The relative stabilities of the two isomers of both $(H_2O)_2^+$ and $(H_2S)_2^+$ are rationalized in terms of the calculated values of the topological properties of the electron density distributions, and it has been observed that one strong bond in the $H_3O^+$ fragment of $(HO\cdots H_3O)^+$ rather than the weak bonds in $(H_2O)_2^+$ play an important role in the underestimation of the stability of

the proton-transferred structure as predicted by DFT. Similarly, in the case of $(H_2S)_2^+$, overestimation of the stability of the hemi-bonded isomer relative to the proton-transferred isomer is caused by the underestimation of the strength of the S−H bond in the $H_3S^+$ fragment of $(HS\cdots H_3S)^+$ by DFT.

**Acknowledgment.** We thank Dr. T. Mukherjee and Dr. J. P. Mittal for their kind interest and encouragement.

## References and Notes

(1) Parr, R. G.; Yang, W. *Density Functional Theory of Atoms and Molecules*; Oxford University Press: New York, 1989.
(2) Parr, R. G.; Yang, W. *Annu. Rev. Phys. Chem.* **1995**, *46*, 701.
(3) Pearson, R. G. *Acc. Chem. Res.* **1993**, *26*, 250.
(4) Ghanty, T. K.; Ghosh, S. K. *J. Am. Chem. Soc.* **1994**, *116*, 3943.
(5) Zhou, Z.; Parr, R. G. *J. Am. Chem. Soc.* **1990**, *112*, 5720.
(6) Gill, P. M. W.; Radom, L. *J. Am. Chem. Soc.* **1988**, *110*, 4931.
(7) Sodupe, M.; Oliva, A.; Bertran, J. *J. Am. Chem. Soc.* **1994**, *116*, 8249.
(8) Barnett, R. N.; Landman, U. *J. Phys. Chem.* **1995**, *99*, 17305.
(9) Barnett, R. N.; Landman, U. *J. Phys. Chem. A* **1997**, *101*, 164.
(10) Sodupe, M.; Bertran, J.; Rodriguez-Santiago, L.; Baerends, E. J. *J. Phys. Chem. A* **1999**, *103*, 166.
(11) Ghanty, T. K.; Ghosh, S. K. *J. Phys. Chem. A* **2002**, *106*, 4200.
(12) (a) Scheiner, S. *Annu. Rev. Phys. Chem.* **1994**, *45*, 23. (b) Scheiner, S. *Hydrogen Bonding: A Theoretical Perspective*; Oxford University Press: New York, 1997.
(13) (a) Jeffrey, G. A.; Saenger, W. *Hydrogen Bonding in Biological Structures*; Springer: Berlin, 1991. (b) Jeffrey, G. A. *An Introduction to Hydrogen Bonding*; Oxford University Press: New York, 1997.
(14) Gordon, M. S.; Jensen, J. H. *Acc. Chem. Res.* **1996**, *29*, 536.
(15) Alkorta, I.; Rozas, I.; Elguero, J. *Chem. Soc. Rev.* **1998**, *27*, 163.
(16) Isaacs, E. D.; Shukla, A.; Platzman, P. M.; Hamann, D. R.; Barbiellini, B.; Tulk, C. A. *Phys. Rev. Lett.* **1999**, *82*, 600.
(17) Ghanty, T. K.; Staroverov, V. N.; Koren, P. R.; Davidson, E. R. *J. Am. Chem. Soc.* **2000**, *122*, 1210.
(18) Sodupe, M.; Oliva, A.; Bertran, J. *J. Am. Chem. Soc.* **1995**, *117*, 8416.
(19) Ghanty, T. K.; Ghosh, S. K. Unpublished work.
(20) See, for example: (a) Borden, W. T.; Davidson, E. R. *Acc. Chem. Res.* **1996**, *29*, 67. (b) Roos, B. O. *Acc. Chem. Res.* **1999**, *32*, 137.
(21) Braïda, B.; Hiberty, P. C.; Savin, A. *J. Phys. Chem. A* **1998**, *102*, 7872.
(22) Grüning, M.; Gritsenko, O. V. O.; van Gisbergen, S. J. A.; Baerends, E. J. *J. Phys. Chem. A* **2001**, *105*, 9211.
(23) Bader, R. F. W. *Atoms in Molecules−A Quantum Theory*; Oxford University Press: Oxford, 1990.
(24) Bader, R. F. W.; MacDougall, P. J.; Lau, C. D. H. *J. Am. Chem. Soc.* **1984**, *106*, 1594.
(25) Dobado, J. A.; Martinez-Garcia, H.; Molina, J.; Sundberg, M. R. *J. Am. Chem. Soc.* **1999**, *121*, 3156; **2000**, *122*, 1144.
(26) Macchi, P.; Iverson, B. B.; Sironi, A.; Chakoumakos, B. C.; Larsen, F. K. *Angew. Chem., Int. Ed.* **2000**, *39*, 2719.
(27) Malcolm, N. O. J.; Popelier, P. L. A. *J. Phys. Chem. A* **2001**, *105*, 7638.
(28) Messerschmidt, M.; Wagner, A.; Wong, M. W.; Luger, P. *J. Am. Chem. Soc.* **2002**, *124*, 732.
(29) (a) Nakano, H. *J. Chem. Phys.* **1993**, *99*, 7983. (b) Nakano, H. *Chem. Phys. Lett.* **1993**, *207*, 372.
(30) Schmidt, M. W.; BalDridge, K. K.; Boatz, J. A.; Elbert, S. T.; Gordon, M. S.; Jensen, J. H.; Koseki, S.; Matsunaga, N.; Nguyen, K. A.; Su, S. J.; Windus, T. L.; Dupuis, M.; Montgomery, J. A., Jr. *J. Comput. Chem.* **1993**, *14*, 1347.
(31) Slater, J. C. *Phys. Rev.* **1951**, *81*, 385.
(32) Becke, A. D. *Phys. Rev. A* **1998**, *38*, 3098.
(33) Gill, P. M. W. *Mol. Phys.* **1996**, *89*, 433.
(34) Perdew, J. P.; Burke, K.; Ernzerhof, M. *Phys. Rev. Lett.* **1996**, *77*, 3865; **1997**, *78*, 1396.
(35) Vosko, S. H.; Wilk, L.; Nusair, M. *Can. J. Phys.* **1980**, *58*, 1200.
(36) Lee, C.; Yang, W.; Parr, R. G. *Phys. Rev. B* **1988**, *37*, 785.
(37) (a) Tsuneda, T.; Hirao, K. *Chem. Phys. Lett.* **1997**, *268*, 510. (b) Tsuneda, T.; Suzumura, T.; Hirao, K. *J. Chem. Phys.* **1999**, *110*, 10664.
(38) Becke, A. D. *J. Chem. Phys.* **1993**, *98*, 1372.
(39) Becke, A. D. *J. Chem. Phys.* **1993**, *98*, 5648.
(40) Klieger-Konig, F. W.; Bader, R. F. W.; Tang, T. H. *J. Comput. Chem.* **1982**, *3*, 317.
(41) Hiberty, P. C.; Humbel, S.; Danovich, D.; Shaik, S. *J. Am. Chem. Soc.* **1995**, *117*, 9003.
(42) Benassi, R.; Taddei, F. *Chem. Phys. Lett.* **1993**, *204*, 595.
(43) Silvi, B.; Savin, A. *Nature* **1994**, *371*, 683.
(44) Fourré, I.; Silvi, B.; Sevin, A.; Chevreau, H. *J. Phys. Chem. A* **2002**, *106*, 2561.